Analysis of Microstrip Structures on and near Dielectric Ridges Using an Integral Equation-Mode Matching Technique

A. G. Engel, Jr. and Linda P. B. Katehi

Radiation Laboratory
The University of Michigan
Ann Arbor MI 48109-2122

ABSTRACT

A full-wave technique which uniquely synthesizes well-known integral equation and mode-matching methods is shown to be applicable to the study of propagation in microstrip structures which are on and near dielectric ridges. Coupled microstrips on dielectric ridges and a microstrip near a chip edge are examined to demonstrate the accuracy and utility of this method.

INTRODUCTION

In the sub-mm and THz frequency ranges, excessive ohmic losses preclude the use of microstrip in monolithic circuits. Whether coplanar waveguide, dielectric waveguide, or another type of guiding structure is used in place of microstrip, monolithic circuits apparently will still employ short lengths of complex microstrip structures. These structures will be microstrip, in that they will consist of conducting strips suspended by a dielectric above a ground plane, but they will be mounted on ridges and in the close proximity of other conductors on other ridges. For example, a typical monolithic circuit could utilize a low-loss dielectric ridged waveguide as a transmission line. A passive circuit element such as an inductor could be created from the selective use of conductors in conjunction with the waveguide. A transition to an active device would consist of a conductor mounted on the ridged waveguide. The active device itself may become wide compared to a guided wavelength, and, if the electrodes are placed in a non-planar fashion on the dielectric ridges and valleys which make up the device, then the transverse wave propagation on the device may be significant. Accurate methods must be developed to analyze the propagation in these complex microstrip structures.

Over the past ten years, the characterization of microstrip structures on and near dielectric ridges has been addressed several times. Quasi-static methods such as an integral equation formulation [1] and the rectangular boundary division method [2, 3] have considered an open microstrip on a finite dielectric and shielded microstrip near a chip edge, respectively. In addition, a full-wave mode-matching technique has been applied to the analysis of microslab waveguide [4], and a modified mode-matching technique has been developed to model transverse wave propagation on FET structures [5]. In early 1990, the method of lines [6] was applied to characterize an electro-optic modulator-type structure, a microstrip on a ridged substrate, and, again, a microstrip near a chip edge. Both the mode matching technique and the method of lines are efficient, but suffer when generalized to a three-dimensional structure (such as a microstrip discontinuity) and when applied to open structures.

In this paper, a full-wave technique which uniquely synthesizes well-known integral equation and mode-matching methods is shown to be applicable to the study of microstrip structures on and near dielectric ridges. Compared to the method of lines and the full-wave mode matching analyses, the integral equation-mode matching technique is more complex than the former and similar in complexity to the latter when shielded two-dimensional structures are considered; however, three-dimensional structures may be much more easily characterized by the integral equation-mode matching technique. To introduce this method, two-dimensional structures—specifically, a microstrip near a chip edge and coupled microstrips on ridges—are examined.

THEORY

The general structure is shown in Figure 1. The structure is uniform in the z-direction. The outer walls are perfect electric conductors. Along the y-axis, the structure is divided into two sections at $y = b_1$. Section A is divided into layers along the x-axis at $x = a_i, i = 1, 2, \ldots$. Conducting strips are located parallel to the x-axis. The generalization of this technique to a structure having more than two sections is possible, but, for simplicity, only the two section case is considered here. The y-dimensions of the strips are assumed to be negligible.

The fields, currents and propagation constants of the structure are determined by solving Pocklington's integral equation in the spatial domain. For a two-dimensional structure such as the one under consideration, this integral equation reduces to

$$\bar{E} = \int_{S'} \overline{\overline{G}}_E \cdot \bar{J}\, dS' \qquad (1)$$

where $\overline{\overline{G}}_E$ is the dyadic electric field Green's function associated with the structure, $\bar{J}$ is the current in the conducting strips, and S' represents the surfaces of the conducting

CH2870-4/91/0000-0135$01.00 © 1991 IEEE

strips. The Green's function is the electric field when the conducting strips are replaced with a current line source at (x', y').

A convenient form of the Green's function is derived by considering each section of the structure as a section of inhomogeneous parallel plate waveguide. In each section, the fields consist of infinite sums of TE_x and TM_x modes. The fields away from the source obey the homogeneous wave equation, and may be determined using vector potentials $\bar{A} = a_x(x,y,z)\hat{x}$ and $\bar{F} = f_x(x,y,z)\hat{x}$ via

$$\bar{E} = -j\omega\bar{A} + \frac{1}{j\omega\epsilon\mu}\nabla\nabla\cdot\bar{A} + \frac{1}{\epsilon}\nabla\times\bar{F} \quad (2)$$

$$\bar{H} = \frac{1}{\mu}\nabla\times\bar{A} + j\omega\bar{F} - \frac{1}{j\omega\epsilon\mu}\nabla\nabla\cdot\bar{F} \quad (3)$$

The x-, y- and z-dependencies of a_x and f_x are separable. The z-dependence in all sections is assumed to be of the form $e^{-j\beta z}$.

Application of the boundary conditions at each layer interface and at the upper and lower conducting walls determines the x-dependence of the fields in each layer in a given section. In addition, these boundary conditions generate transcendental equations for the x-directed wavenumbers.

The y-dependence of the fields consists of infinite sums of plane waves. In section A, the fields are of the form

$$E^A \sim \sum_l \left(A_l^+ e^{-jk_{yl}y} + A_l^- e^{jk_{yl}y}\right) \quad (4)$$

where A_l^+ and A_l^- are the mode amplitudes for the l^{th} mode. For convenience in the application of the boundary conditions, the fields in section B are separated into two parts, which are designated the primary and secondary fields. The primary fields consist of plane waves leaving the source in the $\pm y$-direction, i.e.,

$$E_P^B \sim \begin{cases} \sum_l B_{Pl}^- e^{jk_{yl}(y-y')} & y < y' \\ \sum_l B_{Pl}^+ e^{-jk_{yl}(y-y')} & y > y' \end{cases} \quad (5)$$

The boundary conditions at the source ($y = y'$) are satisfied by the primary fields, and the primary field mode amplitudes $B_{Pl}^{\pm}$ are thereby explicitly determined. The secondary fields satisfy the homogeneous wave equation in all regions and consist of plane waves traveling in both directions, i.e.,

$$E_S^B \sim \sum_l \left(B_{Sl}^+ e^{-jk_{yl}y} + B_{Sl}^- e^{jk_{yl}y}\right) \quad (6)$$

The boundary conditions at $y = 0, b_1$ and b are used to generate two equations from which B_{Sl}^+ and B_{Sl}^- are determined.

The first equation for $B_{Sl}^{\pm}$ stems from the boundary conditions at the section interface $y = b_1$ and at the conducting wall $y = 0$. The basic approach for satisfying the boundary conditions at the section interface is mode-matching [7, 8, 9, 10]. A transmission matrix may then theoretically be used to relate the fields at $y = b_1$ to the fields at $y = 0$, but the number of modes necessary for convergence causes numerical instability. A numerically stable approach modifies the classical mode-matching matrix to a scattering matrix [11, 12, 13, 14]. The scattering matrix S for the junction at $y = b_1$ satisfies

$$\begin{bmatrix} A^- \\ B_P^- + B_S^- \end{bmatrix} = [S]\begin{bmatrix} A^+ \\ B_P^+ + B_S^+ \end{bmatrix} \quad (7)$$

where A^-, A^+, B_P^-, B_P^+, B_S^-, and B_S^+ are all column vectors of the form $A^- = [A_1^- \; A_2^- \; \ldots \; A_l^- \; \ldots]^T$. Application of the boundary conditions at $y = 0$ and manipulation of the scattering matrix equation allows $A^{\pm}$ to be eliminated; hence the incident and reflected waves at the section interface are related by the expression

$$B_S^+ = [R](B_P^- + B_S^-) \quad (8)$$

where

$$[R] = S_{22} - S_{21}\left(I + L^2 S_{11}\right)^{-1} L^2 S_{12} \quad (9)$$

$L = \mathrm{diag}\{e^{-jk_{yl}b_1}\}$, and I is the identity matrix.

The boundary conditions at the conducting wall at $y = b$ and manipulation of the matrix equations give an expression for the section B secondary field mode amplitudes B_S^- in terms of $B_P^{\pm}$. B_S^+ may then be determined from equation 8.

Given the x-, y- and z-dependencies of the fields, the components of the Green's function are known and the integral equation may be solved. The current is assumed to be z-directed, and the distribution on the conductors is described with an entire domain Maxwellian basis function which satisfies the edge condition. The method of moments is applied to obtain a matrix equation for the unknown current coefficients. Zeros of the determinant of the matrix determine the propagation constants of the propagating modes; the currents and fields may be subsequently determined from the integral equation.

RESULTS

The software was developed on an Apollo workstation, and the bulk of the calculations were performed on an IBM RS-6000 computer. In all β-value computations presented here, excellent convergence was obtained using 100 TE_x and 100 TM_x modes in each section.

Verification of the software for simple microstrip and coupled microstrip was accomplished by comparing with the multitudinous data available in the literature; excellent agreement was obtained. For a microstrip near a chip edge, results from the integral equation-mode matching method were compared with the theoretical and experimental results given by Thorburn *et al* [6] (Figure 2). The data are generally in good accord, except for a slight offset between the two theoretical curves. The probable cause of the variation is the inability to exactly recreate the conditions given in [6]; very slight changes in d, w, ϵ_r and frequency are sufficient to bring the curve into even better agreement with

the given experimental data. Also relevant to the discrepancy between this work and the previously published results is the asymmetry of the problem with respect to the center of the conductor. As the strip moves closer to the edge of the chip, the asymmetry becomes more significant and the ability of the symmetric Maxwellian function to describe the current distribution on the conductor becomes impaired. Accuracy may be improved by utilizing basis functions which allow asymmetric current, such as higher order Chebyshev polynomials and simple pulses.

The geometry of two coupled microstrips on dielectric ridges is given in Figure 3; characterization of this structure is displayed in Figures 4 and 5. The first plot illustrates the behavior of the even- and odd-mode phase constants for different spacings over a frequency range which is roughly centered at 94 GHz. The second plot shows the data at 94 GHz as a function of spacing and compares the result to coupled microstrip on a continuous substrate. Two salient features may be discerned from these data.

Typical of coupled lines, the even-mode phase constants generally decrease and the odd-mode phase constants generally increase with increasing spacing— i.e., as the lines become farther apart, the even and odd modes decouple and the phase constants tend toward the single-strip value. However, in this case, for $100\mu\text{m} < s < 150\mu\text{m}$, the odd-mode phase constant *decreases* before it begins to increase. At $s = 100\mu\text{m}$, the ridges are contiguous and the strips are together on a single ridge. As s increases to $110\mu\text{m}$, the increasing gap between the ridges causes an increase in coupling over this range, evidenced by the widening disparity between the even- and odd-mode phase constants. As s increases further, the coupling tends to decrease. The range $100\mu\text{m} < s < 150\mu\text{m}$ may therefore be considered a transition region between the case of two strips on a single ridge and the case of two strips on two ridges. The increased coupling in this transition region raises the possibility of a simple microstrip coupler which is enhanced by a small groove placed between the strips.

The data also demonstrate that as the spacing between strips increases, the strips on the ridges tend to decouple faster than the strips on the continuous substrate. This behavior is evidenced by the faster convergence of the β-s curves for the ridged microstrip to the single strip value of $\beta = 2.90k_o$; the β-s curves for the strips on the continuous substrate converge more slowly to the single strip value of $\beta = 3.07k_o$. When increased packing density is a necessity, a structure of this type may be used in place of conventional microstrip.

CONCLUSION

An integral equation-mode matching method useful in the study of microstrip structures on and near dielectric ridges has been presented, and the method was applied to the characterization of a microstrip near a chip edge and coupled microstrip on dielectric ridges. In the future, the method will be developed so that three-dimensional structures as well as structures consisting of more than two sections may be characterized.

ACKNOWLEDGEMENT

This work was supported by the Army Research Office under the URI program, Contract No. DAAL03-87-K-0007.

REFERENCES

[1] C. E. Smith and R. Chang, "Microstrip Transmission Line with Finite-Width Dielectric," *IEEE Trans. Microwave Theory Tech.*, vol. MTT-28, pp. 90–4, February, 1980.

[2] E. Yamashita, K. R. Li, and Y. Suzuki, "Characterization Method and Simple Design Formulas of MCS Lines Proposed for MMIC's," *IEEE Trans. Microwave Theory Tech.*, vol. MTT-35, pp. 1355–62, December, 1987.

[3] E. Yamashita, H. Ohashi, and K. Atsuki, "Characterization of Microstrip Lines near a Substrate Edge and Design Formulas of Edge-Compensated Microstrip Lines," *IEEE Trans. Microwave Theory Tech.*, vol. MTT-37, pp. 890–6, May, 1989.

[4] B. Young and T. Itoh, "Analysis and Design of Microslab Waveguide," *IEEE Trans. Microwave Theory Tech.*, vol. MTT-35, pp. 850–7, September, 1987.

[5] W. Heinrich and H.L. Hartnagel, "Wave Propagation on MESFET Electrodes and Its Influence on Transistor Gain," *IEEE Trans. Microwave Theory Tech.*, vol. MTT-35, pp. 1–8, January, 1987.

[6] M. Thorburn, A. Agoston, and V. K. Tripathi, "Computation of Frequency-Dependent Propagation Characteristics of Microstriplike Propagation Structures with Discontinuous Layers," *IEEE Trans. Microwave Theory Tech.*, vol. MTT-38, pp. 148–153, February, 1990.

[7] U. Crombach, "Analysis of Single and Coupled Rectangular Dielectric Wave-guides," *IEEE Trans. Microwave Theory Tech.*, vol. MTT-29, pp. 870–4, September, 1981.

[8] R. Mittra, Y. Hou and V. Jamnejad, "Analysis of Open Dielectric Waveguides Using Mode-Matching Techniques and Variational Methods," *IEEE Trans. Microwave Theory Tech.*, vol. MTT-28, pp. 36–43, January, 1980.

[9] K. Solbach and I. Wolff, "The Electromagnetic Fields and The Phase Constants of Dielectric Image Lines," *IEEE Trans. Microwave Theory Tech.*, vol. MTT-26, pp. 266–74, April, 1978.

[10] R. Mittra and S. W. Lee, *Analytical Techniques in the Theory of Guided Waves*. New York: McGraw-Hill, 1961.

[11] R. Safavi-Naini and R. H. MacPhie, "On Solving Waveguide Junction Scattering Problems by the Conservation of Complex Power Technique," *IEEE Trans. Microwave Theory Tech.*, vol MTT-29, pp. 337–43, April, 1981.

[12] R. Safavi-Naini and R. H. MacPhie, "Scattering at Rectangular-to-Rectangular Waveguide Junctions," *IEEE Trans. Microwave Theory Tech.*, vol. MTT-30, pp. 2060–3, November, 1982.

[13] R. R. Mansour and R. H. MacPhie, "Scattering at an N-Furcated Parallel-Plate Waveguide-Junction," *IEEE Trans. Microwave Theory Tech.*, vol. MTT-33, pp. 337–43, September, 1985.

[14] R. R. Mansour and R. H. MacPhie, "An Improved Transmission Matrix Formulation of Cascaded Discontinuities and its Application to E-Plane Circuits," *IEEE Trans. Microwave Theory Tech.*, vol. MTT-34, pp. 1490–8, December, 1986.

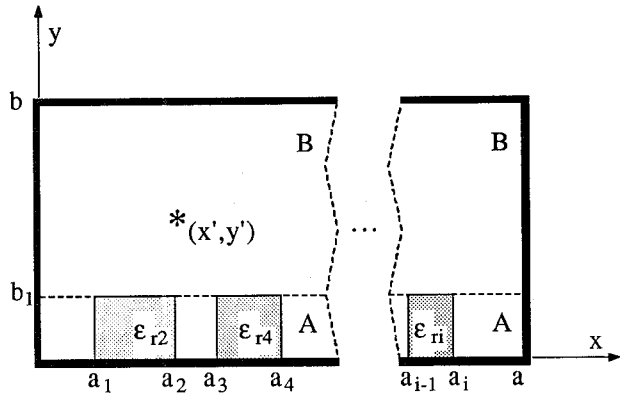

Figure 1: Geometry of the general structure.

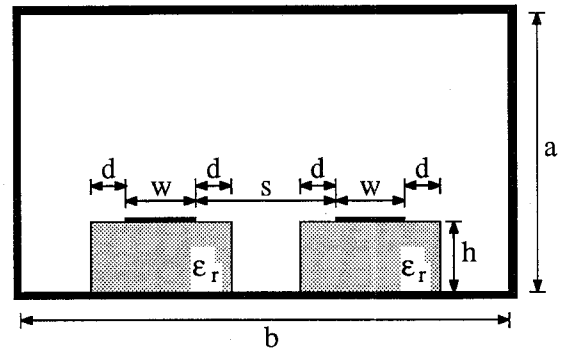

Figure 3: Geometry of two coupled microstrips on dielectric ridges: $w = 0.1$mm, $h = 0.1$mm, $d = 0.05$mm, $a = 1.3$mm, $b = 2.51$mm, and $\epsilon_r = 12.85$.

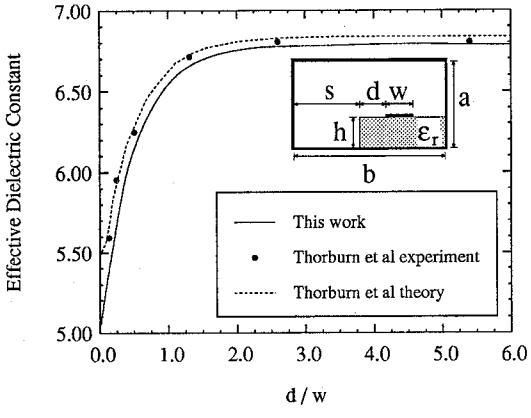

Figure 2: Comparison of this work to reference [6] in the calculation of effective dielectric constant ($\equiv (\beta/k_o)^2$) vs. distance from the strip to the chip edge. Referring to the inset, $\epsilon_r = 10.2$, $w = 0.925$mm, $h = 1.27$mm, $a = 50.0$mm, $b = 35.0$mm, $s = 15.0$mm, and frequency = 2 GHz.

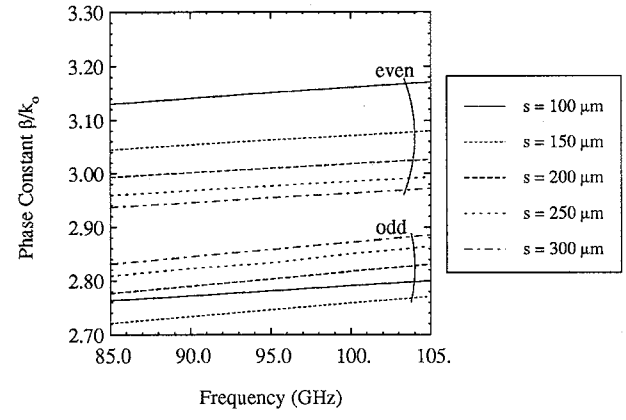

Figure 4: Phase constant vs. frequency at various spacings for the structure described in Figure 4.

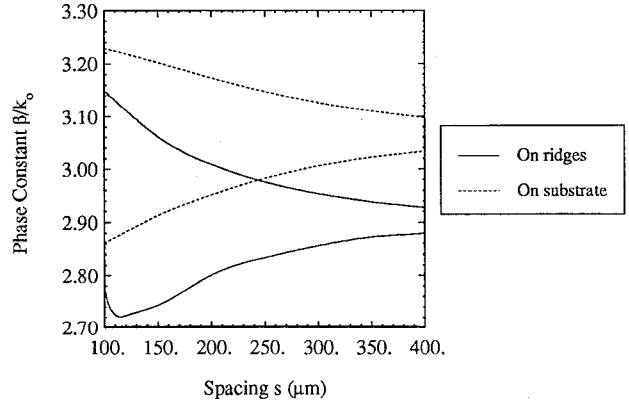

Figure 5: Phase constant vs. spacing at 94 GHz for microstrip on dielectric ridges (Figure 4) and microstrip on continuous substrate (Figure 4, with the two ridges replaced by a single substrate which extends over the entire width of the structure).